

Graphendofullerene: a novel molecular two-dimensional ferromagnet

Diego López-Alcalá¹, Ziqi Hu² and José J. Baldoví^{1,*}

¹Instituto de Ciencia Molecular, Universitat de València, 46980 Paterna, Spain.

²Key Laboratory of Precision and Intelligent Chemistry, Collaborative Innovation Center of Chemistry for Energy Materials (iChEM), Department of Materials Science and Engineering, University of Science and Technology of China, Hefei 230026, China.

E-mail: j.jaime.baldovi@uv.es

ABSTRACT: Carbon chemistry has attracted a lot of attention by chemists, physicists and material scientists in the last decades. The recent discovery of graphullerene provides a promising platform for many applications due to its exceptional electronic properties and the possibility to host molecules or clusters inside the fullerene units. Herein, we introduce graphendofullerene, a novel molecular-based two-dimensional (2D) magnetic material formed by trimetallic nitrides clusters encapsulated on graphullerene. Through first-principles calculations, we demonstrate the successful incorporation of the molecules into the 2D network formed by C₈₀ fullerenes, which leads to a robust long-range ferromagnetic order with a Curie temperature (T_c) of 38 K. Additionally, we achieve a 45% increase in T_c by strain engineering. These findings open the way for a new family of molecular 2D magnets based on graphendofullerene for advanced technologies.

KEYWORDS: 2D magnetism, graphullerene, endohedral fullerenes, carbon allotropes, spintronics

Since the mid of the 80s carbon chemistry has emerged as a prominent research field due to the discovery of synthetic carbon allotropes as fullerenes^{1,2} and carbon nanotubes,³ and the isolation of graphene in 2004,^{4,5} thus offering countless possibilities for exploiting different physical phenomena.⁶ This is due to the different orbital hybridization and arrangement that confer them unique optical and electronic properties. In particular, graphene pioneered the field of 2D materials that nowadays covers a wide range of functionalities,^{7,8} from insulators⁹ to superconductors¹⁰ and magnetic systems,¹¹ leading to applications in catalysis,¹² gas sensing,¹³ valleytronics¹⁴ and spintronics.¹⁵ Moreover, they can be assembled into van der Waals (vdW) heterostructures,¹⁶ and their layers can be twisted with respect to each other, to create novel multifunctional materials and devices.¹⁷

Fullerenes stand out due to their advanced applications in photovoltaics,¹⁸ biomedicine^{19,20} or catalysis.²¹ These arise from their structural morphology, which allows to harbor small molecules or clusters inside the carbon backbone,^{22–24} forming the so-called endohedral fullerenes or metallofullerenes.^{25,26} Due to their heterogeneous nature, these systems have an enormous potential in cutting-edge technologies such as information storage^{27–29} or spintronics.^{30–34} Very recently, a 2D fullerene-based material equivalent to graphene, the so-called graphullerene, has been synthesized.^{35,36} Graphullerene's structure consists of a 2D network of fullerenes covalently interconnected, which provides the system with robust structural stability,^{37,38} and remarkable electronic,^{39–42} mechanical^{43–46} and optical^{47,48} properties. This makes graphullerene well suited as an exciting platform for many different technological applications.^{49–51} However, the capability of the fullerene building blocks as host structures within the 2D network still remains unexplored, even from a theoretical point

of view, which would open infinite possibilities emerging from the versatility of chemistry, in the 2D limit.

In this Letter, we report a first-principles study on a novel 2D material that we name ‘graphendofullerene’ by analogy to graphullerene and endohedral fullerene. The graphullerene-based material that we propose as a proof of concept is formed by magnetic endohedral metallofullerene cages ($V_3N@C_{80}$) as building blocks. First, we demonstrate the thermodynamic stability of graphendofullerene and calculate its electronic structure, magnetic properties and spin dynamics. Interestingly, our microscopic analysis reveals that intermolecular magnetic interactions in the network lead to long-range ferromagnetic order. Finally, we apply strain engineering to enhance the magnetic behavior of the system. Our results pave the way to the preparation of magnetic graphullerene-based materials and their future optimization for emerging applications, since a wide range of possibilities arise from the host capabilities of fullerene building blocks.

C_{60} is the smallest fullerene which obeys the isolated pentagonal ring (IPR) rule,⁵² but its reduced inner space limits the incorporation of a wide variety of guest molecules. This limitation is overcome by C_{80} , the next member that follows IPR rule in the fullerene family with the same point group symmetry (I_h), due to its larger volume.⁵³ Therefore, we create a 2D C_{80} graphullerene network in which each fullerene cage is surrounded by six neighboring cages (Figure S1a), as it has been predicted to be the most stable among all possible configurations.⁵⁴ This structure corresponds to a hexagonal lattice with a $Pmna$ (No. 53) space group, where the fully optimized lattice parameters are $a = 17.84 \text{ \AA}$ and $b = 10.29 \text{ \AA}$. The chemical bonds between adjacent cages are based on [2+2] cycloaddition along a and b lattice vectors and diagonal lines of the rectangular unit cell. Covalent

intramolecular C-C σ bonds have a length of 1.42 Å, whereas intermolecular bonds are 1.59 Å, owing to the novel sp^3 character of the C attaching C_{80} cages. This kind of arrangement maximizes the C sp^3 atoms in the structure, which releases surface tension and stabilizes the entire system.⁵⁵ Our calculations show that the fullerene units are slightly distorted after polymerization, where the cages adopt an ellipsoidal shape, as we can observe in Figure S1b. The calculated out-of-plane diameter of the cages is 8 Å, whereas in the equatorial plane is 8.9 Å, thus having enough space to harbor small molecular species inside them.

In order to evaluate the effect of the encapsulated molecules or clusters on C_{80} graphullerene, we first simulate the electronic structure of the pristine material. Our simulations predict a small band gap of 0.1 eV located at Γ (Figure S1c), which is smaller than the one found in its C_{60} counterpart.⁴¹ A robust hybridization between the σ skeleton and the delocalized π system is present, where the overlap between these energy levels is noticeable (Figure S1c). The π -electron system is delocalized all over the C_{80} cages throughout the aromaticity of the fullerene units while the C atoms acting as linkers show a noticeable electronic localization due to the adopted sp^3 configuration due to the polymerization of the network (Figure S2). This robust interplay between highly ordered arrangement and emerging electronic properties provides an ideal structure for further functionalization and exploration of emergent phenomena upon the introduction of additional molecular components inside of the fullerene units. Note that although the small HOMO-LUMO gap makes the synthesis of pristine I_h - C_{80} unfeasible, the encapsulation of metals inside fullerene cages stabilizes the system. This is due to charge transfer between the embedded species and the fullerene, leading to highly stable endohedral metallofullerenes that do possess a large HOMO-LUMO gap.^{56,57}

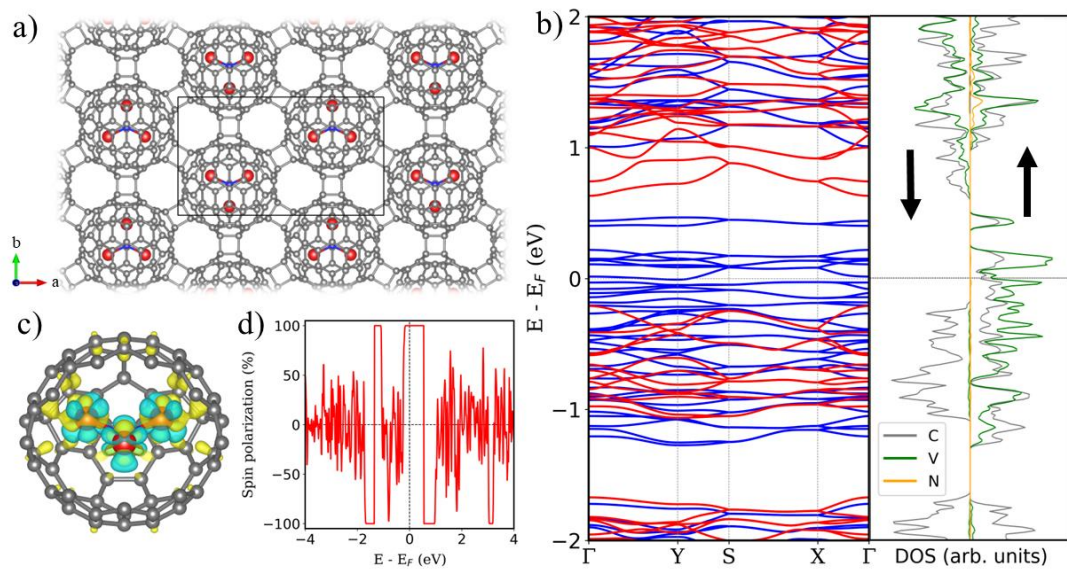


Figure 1: **a)** V₃N@C₈₀ graphendofullerene top view. Color code: carbon (grey), vanadium (blue) and nitrogen (red). **b)** Electronic band structure (left) and projected density of states (PDOS) (right) for V₃N@C₈₀ monolayer. Blue (red) color in a) represents spin up (down) electrons. **c)** Charge density difference after V₃N encapsulation. Yellow (blue) regions represent charge accumulation (depletion). **d)** Energy levels polarization of C₈₀.

Encapsulation of trimetallic nitrides has been demonstrated to be a powerful methodology to stabilize highly symmetric icosahedral fullerenes.^{58,59} Given that, we explore the feasibility of incorporating V₃N into fullerene units⁶⁰ that form a 2D graphullerene network. Thus, we fully optimized the atomic positions and lattice parameters of the V₃N@C₈₀ network, where the guest clusters adopt a conformation pointing towards half of the sp³ bridges in a C₃-symmetry fashion (Figure 1a). We can see that the clusters present a slight distortion from planarity, due to unpaired electrons in N, but they mostly lay at the network plane. Also, the incorporation of the clusters barely distorts the fullerene cages, where the average host-guest distance is ~2.5 Å, which is compatible

with a van der Waals interaction. Then, we calculate the formation energy (E_F), that is defined as $E_F = E_{V_3N@C_{80}} - (E_{V_3N} + E_{C_{80}})$. We found an E_F of -10.73 eV/molecule that is compatible with similar theoretical studies for the endohedral metallofullerene cages.⁶¹ This indicates a favorable formation of the $V_3N@C_{80}$ network, because the system is stabilized with respect to its separate V_3N and C_{80} units. A charge transfer of 2.4 e per V_3N cluster to the graphullerene network is revealed by Bader charge analysis, where the V atoms are the responsible to donate charge density to the C skeleton (Figure 1c). Furthermore, in order to corroborate the stability of the detailed graphendofullerene, we performed *ab initio* molecular dynamics (AIMD) calculations to monitor the dynamical stability of the system at a given temperature. Our calculations unveil that the structure is thermodynamically stable at room temperature and up to 600 K (Figure S3).

The electronic band structure and density of states of the $V_3N@C_{80}$ network is shown in Figure 1b. One can observe a clear influence of the host-guest interaction due to strong spin-dependent hybridization between energy levels around the Fermi energy due to the charge transfer interaction. Consequently, the energy levels of C atoms on the network are polarized due to the interaction with magnetic clusters, as illustrated in Figure 1d. This interaction is responsible for redistributing the charge density of the system after encapsulation and harnessing the stabilization of the network.

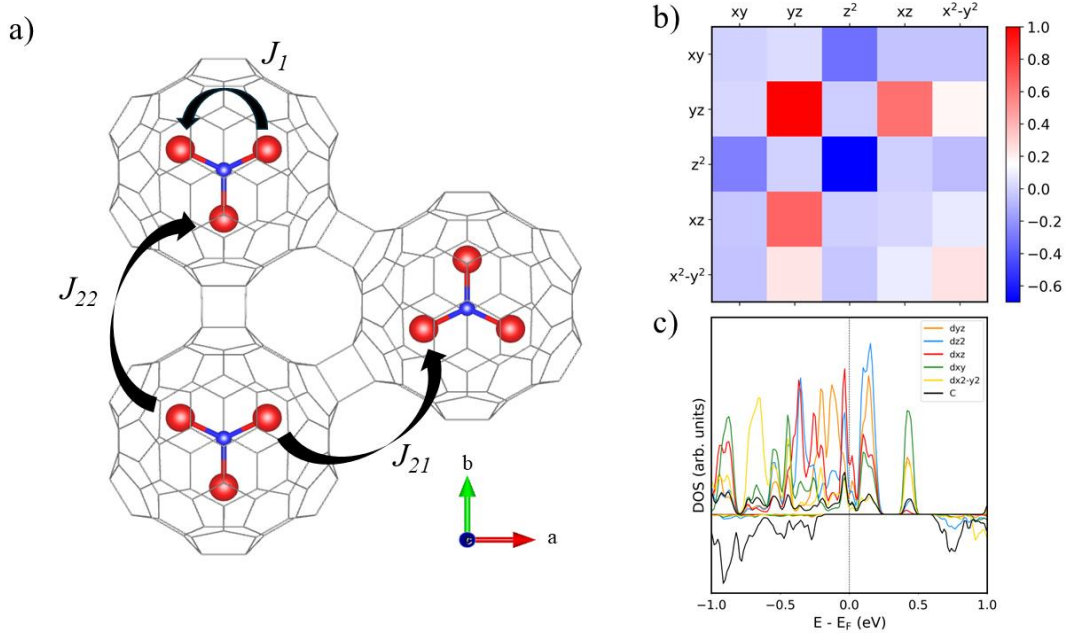


Figure 2. a) Schematic representation of intra/intermolecular magnetic interactions in V₃N@C₈₀ network. b) Orbital contribution to J_{21} from first neighbor V atoms interacting. c) PDOS of d orbitals of V atoms in J_{21} and C atoms in linking moieties of V₃N@C₈₀.

Once the thermodynamic and electronic properties of V₃N@C₈₀ network are elucidated, we systematically study the magnetic properties of graphendofullerene as a novel molecule-based 2D magnet. The calculated magnetic moments are 2.7 μ_B for V atoms, whereas the long-range magnetic order present in the monolayer is predicted to be ferromagnetic, as $E_{FM} - E_{AFM} = 0.23$ eV. Regarding magnetic exchange interactions (J), the arrangement of C₈₀ cages and the morphology of the guest clusters allow several J s in the network (Figure 2a). We categorize them into two different groups, namely: (i) intramolecular interactions, *i.e.* those interactions between V atoms from the same molecule (J_1) and, (ii) intermolecular interactions, which are those magnetic interactions between adjacent molecules in the network (J_2). Due to the close distance between V atoms forming guest clusters (~ 3.2 Å), J_1 interactions have a high intensity of ~ 50 meV and short-range intrinsic character, mainly due to a robust hybridization of d orbitals

around Fermi level that enhances magnetic intramolecular interactions (Figure 2c) but prevents the participation of J_1 in the magnetic reciprocity of the network. These intramolecular interactions stabilize a ferromagnetic coupling between the V atoms inside the guest molecules. On the other hand, the main factor in the stabilization of a long-range magnetic order in the graphendofullerene are intermolecular ferromagnetic exchange interactions between adjacent V_3N molecules. The orientation of guest clusters inside C_{80} cages provides two different first neighbor intermolecular interactions, namely, J_{21} , that arises from the V atoms directly oriented along the x axis of the network, and J_{22} , which is aligned to y axis. In the case of J_{21} , the V atoms point directly towards them, and the resulting interaction at 6.7 Å is 2.28 meV, whereas J_{22} is equal to 0.33 meV due to a longer distance of interaction (7.8 Å). J_{21} (J_{22}) are one (two) order of magnitude lower than J_1 but connect magnetic molecules and provides the $V_3N@C_{80}$ network with a robust long-range magnetic order, that opens the way to observe critical properties of a ferromagnet as a Curie temperature (T_c) or coercivity on this molecule-based 2D network.

In order to check the role of C_{80} graphullerene on the mediation of intermolecular magnetic exchange coupling, we recomputed the magnetic exchange interactions in a free-standing molecular array (i.e. removing all C atoms from the calculation). We found that intermolecular interactions are suppressed, whereas J_1 remains present (See Figure S4). This result is a useful hint that points to the carbon skeleton as mediator of the magnetic interactions that stabilize ferromagnetism in the network. Our calculations reveal that intermolecular interactions are mainly governed by a ferromagnetic d_{yz} - d_{yz} contribution, with moderate d_{xz} - d_{yz} and d_{yz} - d_{xz} ferromagnetic and d_z^2 - d_z^2 antiferromagnetic pathways, between adjacent V atoms (Figure 2b). The influence of these d orbitals is mainly governed by their hybridization with the p orbitals of C atoms in the linking

moieties. Around Fermi level, the contributions of d_{yz} , d_{xz} and d_z^2 are dominant and their hybridization with the energy levels of C atoms that link the C_{80} cages is deduced (Figure 2c). One can notice that this is the main factor in the mediation of intermolecular magnetic interactions.

Subsequently, we performed well-converged spin-orbit calculations in $V_3N@C_{80}$ graphendofullerene to elucidate the preferential spin orientation. We computed the magnetic anisotropy energy (MAE) as the difference in energy in the different possible spin orientations along Cartesian axis. We found 0.18 and 0.15 meV/atom MAE for the spin pointing along x and y axis, with respect to the off-plane direction z , respectively. These results indicate favorable in-plane spin orientation.

To further understand the magnetic behavior of graphendofullerene we performed atomistic spin dynamics simulations. This approach offers a deeper investigation of the more complex magnetic interactions at play, revealing dynamic behaviors that extend beyond the static properties previously described. We predict a T_c of 38 K for $V_3N@C_{80}$ graphendofullerene (Figure 3a), which is similar to that observed in the well-studied 2D ferromagnet CrI_3 .⁶² Although this value is still far from room temperature, the interplay between molecular design and intricate magnetic phenomena presents a fertile ground for future enhancements. We also simulated T_c by only considering J_I interactions, which result in a suppression of ferromagnetism above 0 K (Figure S5). This unveils the critical role of intermolecular interactions on the stabilization of long-range magnetic order in the network.

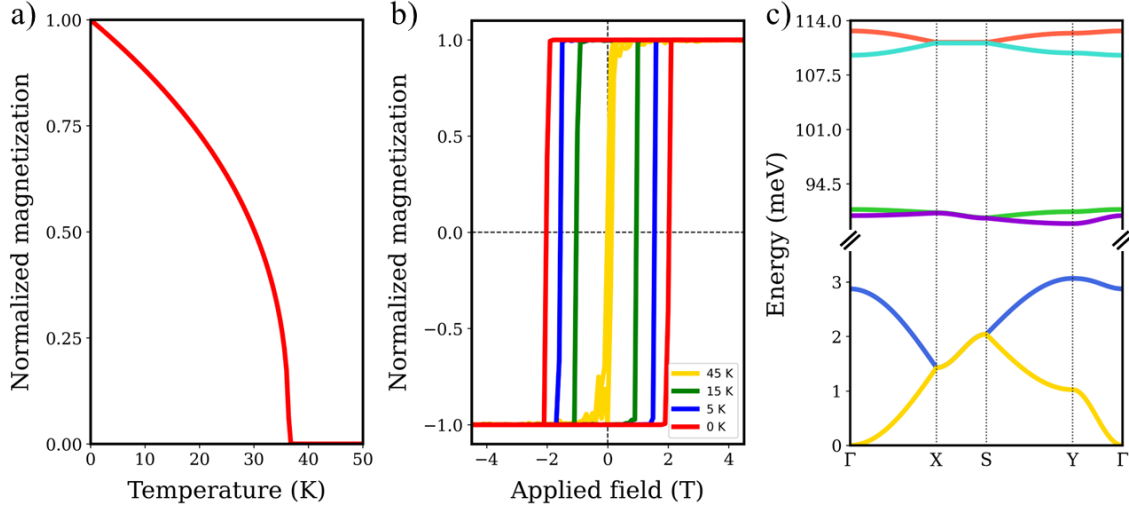


Figure 3: Simulated **a)** hysteresis loop at different temperatures, **b)** Curie temperature and **c)** magnon dispersion for $V_3N@C_{80}$ graphendofullerene network.

We next focus on two key aspects that further highlight the magnetic performance for future applications of $V_3N@C_{80}$ graphendofullerene: the hysteresis loop and magnon dispersion. Firstly, we focus on the magnetic hysteresis behavior of the network, which indicates the relationship between an applied magnetic field (B) and the magnetization of the system. We compute it at different temperatures to simulate the effect of thermal fluctuations until T_c is exceeded (Figure 3b). These findings support the results observed in critical temperature simulations, as the evolution of temperature is closing the loop revealing the transition from the ferromagnetic to paramagnetic order at temperatures above T_c . Besides, we found a coercive field (H_c) of 2 T at 0 K, which is consistent with the expected value of 2.34 T following the classical H_c limit as $H_c \approx 2K/\mu_0 M_s$, where K being the magnetic anisotropy, μ_0 is the vacuum permeability and M_s is the saturation magnetization.

From the calculated magnetic exchange couplings, we simulate the spin-wave spectrum of $V_3N@C_{80}$ graphendofullerene using the Holstein–Primakoff transformation as

introduced by linear spin-wave theory (LSWT) (Figure 3c). At high frequencies, we can observe four magnon bands (between ~ 90 and ~ 115 meV) dominated by J_1 , which are the strongest magnetic interactions in the material and localized inside the guest molecules. On the other hand, the two magnon bands that have more contribution of J_2 interactions are lying at lower energies (between 0 and ~ 3 meV) due to the less intense character of these intermolecular interactions. Arising from the anisotropy of the magnetic exchange interactions, we observe a higher dispersion of spin excitations in the $\Gamma - X$ and $S - Y$ k-paths (corresponding to x axis in real space). This observation matches the magnetic picture described above, as we predict that J_{21} interactions stabilize the ferromagnetic order in the network and this magnetic interaction takes place along x axis.

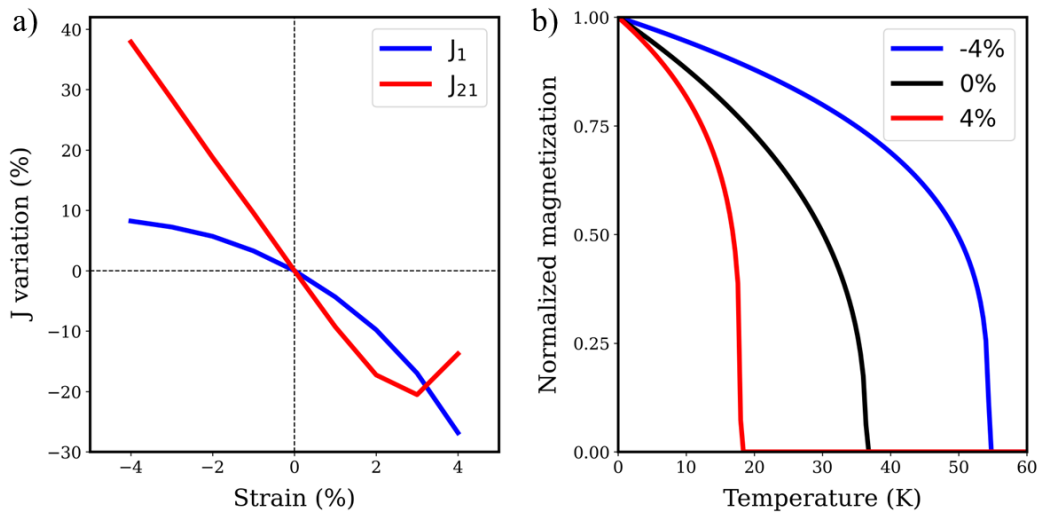


Figure 4: Evolution with strain of **a)** intra/intermolecular magnetic exchange couplings and **b)** Curie temperature of $V_3N@C_{80}$ graphendofullerene.

Then, we explore the effect of mechanical deformation in $V_3N@C_{80}$ monolayer. For that, we recomputed the magnetic properties of the system in a reasonable range of $\pm 4\%$ of biaxial strain. Figure 4a shows the variation of first neighbor inter/intramolecular

interactions upon mechanical deformation. As any mechanical deformation of the lattice will affect the distance between the C₈₀ cages, J_{2I} is critically affected by strain, since this interaction mainly depends on the communication between fullerene units. On the other hand, one may observe that intramolecular interactions are affected to a much lesser extent. According to our calculations, a biaxial compression of the lattice parameters up to 4% would enhance the strength of magnetic exchange interactions by 8% and 37% for J_I and J_{2I} , respectively. With respect to the calculated trend of J_{2I} upon strain, we can observe a deviation from linearity at elongations close to 4%, owing to a competition between FM and AFM orders that appears due to the larger distance between magnetic molecules. We can assert that the enhancement of J_{2I} is mainly due to a higher overlap between d_{xz} and d_{yz} with the C sp³ linkers between cages, as any other competing pathway of interaction is playing a role. We corroborate this fact by looking at the orbital contributions to magnetic exchange couplings, where the same picture is observed compared to the former case (Figure S6). In the case of J_I , the increased intensity is driven by stronger intramolecular interactions, as the reduced volume of the fullerene brings the atoms inside the cage closer. By contrast, when positive strain is applied, we observe a distinct shift in the magnetic behavior of the system. As the lattice expands, the intermolecular distances between C₈₀ cages increase, weakening the magnetic interactions. This reduction in coupling strength leads to a noticeable decrease in both J_I and J_{2I} , highlighting the sensitivity of these interactions to tensile strain.

Obviously, this change in magnetic interactions has a direct impact on the T_c of the system. Figure 4b shows the evolution of T_c of V₃N@C₈₀ graphendofullerene as a function of strain. As magnetic interactions weaken under elongation, T_c is critically diminished, indicating a loss of magnetic ordering at lower temperatures. However, the

opposite picture comes with the application of negative strain. Our results show that compressive strain leads to a significant increase in T_c , which rises up to 55 K within a 4% compression of the 2D molecular ferromagnetic network.

Finally, we also test the influence on the magnetic properties of substituting V by Sc atoms in the trimetallic nitride molecules, as endohedral metallofullerenes based on Sc_3N , VSc_2N and V_2ScN have already been synthesized.⁵⁹ In particular, we determine the magnetic exchange interactions using two structural models (Figure S7a and S8a) based on $\text{V}_2\text{ScN}@C_{80}$ graphendofullerene, as the introduction of the Sc atoms induces structural anisotropy in the network depending on molecular orientations. Our simulations reveal that, contrary to V_3N , antiferromagnetic coupling between adjacent molecules is favored, and a decrease of the absolute strength of both intra- and intermolecular magnetic coupling takes place (Figures S7(b-d) and S8(b-d)). However, the introduction of Sc atoms does not quench long-range magnetism in the system, which may encourage the experimental preparation of magnetic $\text{V}_2\text{ScN}@C_{80}$ graphendofullerene.

The present work represents the first investigation on the functionalization of graphullerene, by using endohedral metallofullerenes, to induce and tailor magnetic properties at the 2D limit. Taking advantage of the versatility of the chemical approach that we propose within the design of this system, there are infinite possibilities arising from the use of fullerenes as building blocks to create new graphendofullerenes with promising future perspectives both from fundamental and applications point of view. The family of fullerenes is constituted by a wide variety of compounds with a broad range of sizes and geometries. The further polymerization of these building blocks into graphullerene structures will pose new challenges to the chemists to create a large range

of 2D carbon-based networks with different host capabilities. On the other hand, the encapsulation of different types of magnetic guest clusters will generate new graphendofullerene networks with a vast range of emerging properties. As we have proven, the interactions between guest clusters can be key for the overall magnetic response of the system. Nowadays the advanced techniques on chemical synthesis of endohedral metallofullerenes lead to the encapsulation of plenty of clusters, mainly containing transition metals and rare-earth ions, which also enhances the potential of metallofullerenes as a versatile platform for the development of chemically robust single molecule-magnets (SMMs).²⁴ Graphendofullerenes can take advantage of this feature representing a promising avenue for emerging phenomena since we have demonstrated that using endohedral metallofullerenes as building blocks stands as a powerful methodology to construct functional materials with enormous potential in optoelectronics, spintronics, magnonics and quantum technologies, among others.

In summary, we introduce graphendofullerene, a two-dimensional magnetic network based on V_3N cluster encapsulated on C_{80} graphullerene, using first principles. Our systematic study provides a detailed understanding of the magnetic properties of $V_3N@C_{80}$ graphendofullerene, which shows a robust ferromagnetic behavior sustained by long-range magnetic interactions enabled by the carbon network. Our atomistic spin simulations reveal that magnetic order can persist up to 38 K and we also determine the hysteresis loop and magnon dispersion of graphendofullerene. Finally, we apply strain engineering that allow to achieve a 45% increase in T_c under the application of 4% compressive strain, evidencing the potential of straintronics in this kind of materials. This work not only bridges molecular chemistry and carbon chemistry but also provides a

versatile platform for the future development of tunable, high-performance next generation molecular-based 2D magnets.

METHODS

Structural relaxations and AIMD were performed using Vienna Ab initio Simulation Package (VASP).^{63,64} The generalized gradient approximation (GGA) with Perdew–Burke–Ernzerhof (PBE) parametrization was used for account for exchange–correlation energy.⁶⁵ Van der Waals interactions were considered using Grimme D3 method approximation.⁶⁶ Projector-augmented wave (PAW) method was used with an energy cutoff of 530 eV. A 5 x 4 x 1 k-point grid was used to sample reciprocal space. Lattice constant and atomics coordinates were relaxed until forces were less than 0.03 eV/Å. *Ab Initio* molecular dynamics (AIMD) were performed following the *NVT* canonical ensemble during 9 ps with a time step of 2 fs. Charge transfer analysis was performed using Bader charge partition as proposed by the Henkelman group.⁶⁷ Magnetic properties were calculated using SIESTA code,^{68,69} in order to take advantage of the localized pseudoatomic orbitals approach. The same k-point grid was used in combination with a real-space mesh cutoff of 700 Ry. We fed TB2J package⁷⁰ with SIESTA wavefunctions to calculate magnetic exchange couplings. We used $H = - \sum_{i \neq j} J_{ij} \vec{S}_i \cdot \vec{S}_j$ as spin Hamiltonian. Atomistic spin dynamics simulations were carried out using Vampire software,⁷¹ where a 30 nm x 30 nm sample was considered in combination with 500000 equilibration and loop time steps.

ASSOCIATED CONTENT

Pristine C₈₀ graphullerene calculations; AIMD simulations; strain engineering of V₃N@C₈₀; V₂ScN@C₈₀ calculations; DFT+U.

AUTHOR INFORMATION

Corresponding Author

*E-mail: j.jaime.baldovi@uv.es.

Author Contributions

This work is part of the PhD thesis of D.L.A. D.L.A. performed the DFT and atomistic spin simulations. Z.H. provided experimental insights and contributed to the interpretation of results. J.J.B. conceived and supervised the work. The manuscript was written by D.L.A. and J.J.B, with contributions of all authors. All authors have given approval to the final version of the manuscript.

Notes

The authors declare no competing financial interest.

ACKNOWLEDGMENTS

The authors acknowledge the financial support from the European Union (ERC-2021-StG101042680 2D-SMARTiES), the Generalitat Valenciana (grant CIDEXG/2023/1), the National Natural Science Foundation of China (52302052) and the Anhui Provincial Natural Science Foundation (2308085MB33).

REFERENCES

- (1) Kroto, H. W.; Heath, J. R.; O'Brien, S. C.; Curl, R. F.; Smalley, R. E. C₆₀: Buckminsterfullerene. *Nature* **1985**, *318* (6042), 162–163.
- (2) Diederich, F.; Ettl, R.; Rubin, Y.; Whetten, R. L.; Beck, R.; Alvare, M.; Anz, S.; Sensharma, D.; Wudl, F.; Khemani, K. C.; Koch, A. The Higher Fullerenes: Isolation and Characterization of C₇₆, C₈₄, C₉₀, C₉₄, and C₇₀O, an Oxide of D_{5h}-C₇₀. *Science* (1979) **1991**, *252* (5005), 548–551.
- (3) Iijima, S. Helical Microtubules of Graphitic Carbon. *Nature* **1991**, *354* (6348), 56–58.
- (4) Novoselov, K. S.; Geim, A. K.; Morozov, S. V.; Jiang, D.; Zhang, Y.; Dubonos, S. V.; Grigorieva, I. V.; Firsov, A. A. Electric Field Effect in Atomically Thin Carbon Films. *Science* (1979) **2004**, *306* (5696), 666–669.

- (5) Geim, A. K.; Novoselov, K. S. The Rise of Graphene. *Nat Mater* **2007**, *6* (3), 183–191.
- (6) Hirsch, A. The Era of Carbon Allotropes. *Nat Mater* **2010**, *9* (11), 868–871.
- (7) Bhimanapati, G. R.; Lin, Z.; Meunier, V.; Jung, Y.; Cha, J.; Das, S.; Xiao, D.; Son, Y.; Strano, M. S.; Cooper, V. R.; Liang, L.; Louie, S. G.; Ringe, E.; Zhou, W.; Kim, S. S.; Naik, R. R.; Sumpter, B. G.; Terrones, H.; Xia, F.; Wang, Y.; Zhu, J.; Akinwande, D.; Alem, N.; Schuller, J. A.; Schaak, R. E.; Terrones, M.; Robinson, J. A. Recent Advances in Two-Dimensional Materials beyond Graphene. *ACS Nano* **2015**, *9* (12), 11509–11539.
- (8) Butler, S. Z.; Hollen, S. M.; Cao, L.; Cui, Y.; Gupta, J. A.; Gutiérrez, H. R.; Heinz, T. F.; Hong, S. S.; Huang, J.; Ismach, A. F.; Johnston-Halperin, E.; Kuno, M.; Plashnitsa, V. V.; Robinson, R. D.; Ruoff, R. S.; Salahuddin, S.; Shan, J.; Shi, L.; Spencer, M. G.; Terrones, M.; Windl, W.; Goldberger, J. E. Progress, Challenges, and Opportunities in Two-Dimensional Materials Beyond Graphene. *ACS Nano* **2013**, *7* (4), 2898–2926.
- (9) Illarionov, Y. Yu.; Knobloch, T.; Jech, M.; Lanza, M.; Akinwande, D.; Vexler, M. I.; Mueller, T.; Lemme, M. C.; Fiori, G.; Schwierz, F.; Grasser, T. Insulators for 2D Nanoelectronics: The Gap to Bridge. *Nat Commun* **2020**, *11* (1), 3385.
- (10) Saito, Y.; Nojima, T.; Iwasa, Y. Highly Crystalline 2D Superconductors. *Nat Rev Mater* **2016**, *2* (1), 16094.
- (11) Gibertini, M.; Koperski, M.; Morpurgo, A. F.; Novoselov, K. S. Magnetic 2D Materials and Heterostructures. *Nat Nanotechnol* **2019**, *14* (5), 408–419.
- (12) Deng, D.; Novoselov, K. S.; Fu, Q.; Zheng, N.; Tian, Z.; Bao, X. Catalysis with Two-Dimensional Materials and Their Heterostructures. *Nat Nanotechnol* **2016**, *11* (3), 218–230.
- (13) Yang, S.; Jiang, C.; Wei, S. Gas Sensing in 2D Materials. *Appl Phys Rev* **2017**, *4* (2).
- (14) Schaibley, J. R.; Yu, H.; Clark, G.; Rivera, P.; Ross, J. S.; Seyler, K. L.; Yao, W.; Xu, X. Valleytronics in 2D Materials. *Nat Rev Mater* **2016**, *1* (11), 16055.
- (15) Ahn, E. C. 2D Materials for Spintronic Devices. *NPJ 2D Mater Appl* **2020**, *4* (1), 17.
- (16) Novoselov, K. S.; Mishchenko, A.; Carvalho, A.; Castro Neto, A. H. 2D Materials and van Der Waals Heterostructures. *Science (1979)* **2016**, *353* (6298).
- (17) Cao, Y.; Fatemi, V.; Fang, S.; Watanabe, K.; Taniguchi, T.; Kaxiras, E.; Jarillo-Herrero, P. Unconventional Superconductivity in Magic-Angle Graphene Superlattices. *Nature* **2018**, *556* (7699), 43–50.
- (18) Li, C.-Z.; Yip, H.-L.; Jen, A. K.-Y. Functional Fullerenes for Organic Photovoltaics. *J Mater Chem* **2012**, *22* (10), 4161.
- (19) Friedman, S. H.; DeCamp, D. L.; Sijbesma, R. P.; Srdanov, G.; Wudl, F.; Kenyon, G. L. Inhibition of the HIV-1 Protease by Fullerene Derivatives: Model Building Studies and Experimental Verification. *J Am Chem Soc* **1993**, *115* (15), 6506–6509.
- (20) Montellano, A.; Da Ros, T.; Bianco, A.; Prato, M. Fullerene C₆₀ as a Multifunctional System for Drug and Gene Delivery. *Nanoscale* **2011**, *3* (10), 4035.
- (21) Pan, Y.; Liu, X.; Zhang, W.; Liu, Z.; Zeng, G.; Shao, B.; Liang, Q.; He, Q.; Yuan, X.; Huang, D.; Chen, M. Advances in Photocatalysis Based on Fullerene C₆₀ and Its Derivatives: Properties, Mechanism, Synthesis, and Applications. *Appl Catal B* **2020**, *265*, 118579.
- (22) Popov, A. A.; Yang, S.; Dunsch, L. Endohedral Fullerenes. *Chem Rev* **2013**, *113* (8), 5989–6113.
- (23) Yang, S.; Wei, T.; Jin, F. When Metal Clusters Meet Carbon Cages: Endohedral Clusterfullerenes. *Chem Soc Rev* **2017**, *46* (16), 5005–5058.
- (24) Hu, Z.; Yang, S. Endohedral Metallofullerene Molecular Nanomagnets. *Chem Soc Rev* **2024**, *53* (6), 2863–2897.
- (25) Kato, H.; Taninaka, A.; Sugai, T.; Shinohara, H. Structure of a Missing-Caged Metallofullerene: La₂@C₇₂. *J Am Chem Soc* **2003**, *125* (26), 7782–7783.
- (26) Wang, C.-R.; Kai, T.; Tomiyama, T.; Yoshida, T.; Kobayashi, Y.; Nishibori, E.; Takata, M.; Sakata, M.; Shinohara, H. C₆₆ Fullerene Encaging a Scandium Dimer. *Nature* **2000**, *408* (6811), 426–427.
- (27) Westerström, R.; Dreiser, J.; Piamonteze, C.; Muntwiler, M.; Weyeneth, S.; Brune, H.; Rusponi, S.; Nolting, F.; Popov, A.; Yang, S.; Dunsch, L.; Greber, T. An Endohedral

- Single-Molecule Magnet with Long Relaxation Times: DySc₂N@C₈₀. *J Am Chem Soc* **2012**, *134* (24), 9840–9843.
- (28) Liu, F.; Gao, C.-L.; Deng, Q.; Zhu, X.; Kostanyan, A.; Westerström, R.; Wang, S.; Tan, Y.-Z.; Tao, J.; Xie, S.-Y.; Popov, A. A.; Greber, T.; Yang, S. Triangular Monometallic Cyanide Cluster Entrapped in Carbon Cage with Geometry-Dependent Molecular Magnetism. *J Am Chem Soc* **2016**, *138* (44), 14764–14771.
- (29) Liu, F.; Krylov, D. S.; Spree, L.; Avdoshenko, S. M.; Samoylova, N. A.; Rosenkranz, M.; Kostanyan, A.; Greber, T.; Wolter, A. U. B.; Büchner, B.; Popov, A. A. Single Molecule Magnet with an Unpaired Electron Trapped between Two Lanthanide Ions inside a Fullerene. *Nat Commun* **2017**, *8* (1), 16098.
- (30) Wang, T.; Wu, J.; Xu, W.; Xiang, J.; Lu, X.; Li, B.; Jiang, L.; Shu, C.; Wang, C. Spin Divergence Induced by Exohedral Modification: ESR Study of Sc₃C₂@C₈₀ Fullerypyrrolidine. *Angewandte Chemie International Edition* **2010**, *49* (10), 1786–1789.
- (31) Feng, Y.; Wang, T.; Li, Y.; Li, J.; Wu, J.; Wu, B.; Jiang, L.; Wang, C. Steering Metallofullerene Electron Spin in Porous Metal–Organic Framework. *J Am Chem Soc* **2015**, *137* (47), 15055–15060.
- (32) Ma, Y.; Wang, T.; Wu, J.; Feng, Y.; Jiang, L.; Shu, C.; Wang, C. Susceptible Electron Spin Adhering to an Yttrium Cluster inside an Azafullerene C₇₉N. *Chemical Communications* **2012**, *48* (94), 11570.
- (33) Wu, B.; Wang, T.; Feng, Y.; Zhang, Z.; Jiang, L.; Wang, C. Molecular Magnetic Switch for a Metallofullerene. *Nat Commun* **2015**, *6* (1), 6468.
- (34) Kurihara, H.; Iiduka, Y.; Rubin, Y.; Waelchli, M.; Mizorogi, N.; Slanina, Z.; Tsuchiya, T.; Nagase, S.; Akasaka, T. Unexpected Formation of a Sc₃C₂@C₈₀ Bisfulleroid Derivative. *J Am Chem Soc* **2012**, *134* (9), 4092–4095.
- (35) Meirzadeh, E.; Evans, A. M.; Rezaee, M.; Milich, M.; Dionne, C. J.; Darlington, T. P.; Bao, S. T.; Bartholomew, A. K.; Handa, T.; Rizzo, D. J.; Wiscons, R. A.; Reza, M.; Zangiabadi, A.; Fardian-Melamed, N.; Crowther, A. C.; Schuck, P. J.; Basov, D. N.; Zhu, X.; Giri, A.; Hopkins, P. E.; Kim, P.; Steigerwald, M. L.; Yang, J.; Nuckolls, C.; Roy, X. A Few-Layer Covalent Network of Fullerenes. *Nature* **2023**, *613* (7942), 71–76.
- (36) Hou, L.; Cui, X.; Guan, B.; Wang, S.; Li, R.; Liu, Y.; Zhu, D.; Zheng, J. Synthesis of a Monolayer Fullerene Network. *Nature* **2022**, *606* (7914), 507–510.
- (37) Shen, G.; Li, L.; Tang, S.; Jin, J.; Chen, X.-J.; Peng, Q. Stability and Elasticity of Quasi-Hexagonal Fullerene Monolayer from First-Principles Study. *Crystals (Basel)* **2023**, *13* (2), 224.
- (38) Peng, B. Stability and Strength of Monolayer Polymeric C₆₀. *Nano Lett* **2023**, *23* (2), 652–658.
- (39) Tromer, R. M.; Ribeiro, L. A.; Galvão, D. S. A DFT Study of the Electronic, Optical, and Mechanical Properties of a Recently Synthesized Monolayer Fullerene Network. *Chem Phys Lett* **2022**, *804*, 139925.
- (40) Argaman, U.; Makov, G. Structure and Properties of Graphullerene: A Semiconducting Two-Dimensional C₆₀ Crystal. *NPJ Comput Mater* **2023**, *9* (1), 211.
- (41) Capobianco, A.; Wiktor, J.; Landi, A.; Ambrosio, F.; Peluso, A. Electron Localization and Mobility in Monolayer Fullerene Networks. *Nano Lett* **2024**, *24* (27), 8335–8342.
- (42) Cassiano, T. S. A.; Pereira, M. L.; e Silva, G. M.; de Oliveira Neto, P. H.; Ribeiro, L. A. Large Polarons in Two-Dimensional Fullerene Networks: The Crucial Role of Anisotropy in Charge Transport. *Nanoscale* **2024**, *16* (5), 2337–2346.
- (43) Zhao, S.; Zhang, X.; Ni, Y.; Peng, Q.; Wei, Y. Anisotropic Mechanical Response of a 2D Covalently Bound Fullerene Lattice. *Carbon N Y* **2023**, *202*, 118–124.
- (44) Ying, P.; Dong, H.; Liang, T.; Fan, Z.; Zhong, Z.; Zhang, J. Atomistic Insights into the Mechanical Anisotropy and Fragility of Monolayer Fullerene Networks Using Quantum Mechanical Calculations and Machine-Learning Molecular Dynamics Simulations. *Extreme Mech Lett* **2023**, *58*, 101929.
- (45) Yu, L.; Xu, J.; Peng, B.; Qin, G.; Su, G. Anisotropic Optical, Mechanical, and Thermoelectric Properties of Two-Dimensional Fullerene Networks. *J Phys Chem Lett* **2022**, *13* (50), 11622–11629.

- (46) Ying, P.; Hod, O.; Urbakh, M. Superlubric Graphullerene. *Nano Lett* **2024**, *24* (34), 10599–10604.
- (47) Champagne, A.; Camarasa-Gómez, M.; Ricci, F.; Kronik, L.; Neaton, J. B. Strongly Bound Excitons and Anisotropic Linear Absorption in Monolayer Graphullerene. *Nano Lett* **2024**, *24* (23), 7033–7039.
- (48) Yuan, D.; Pi, H.; Jiang, Y.; Hu, Y.; Zhou, L.; Jia, Y.; Su, G.; Fang, Z.; Weng, H.; Ren, X.; Zhang, W. Highly In-Plane Anisotropic Optical Properties of Fullerene Monolayers. *Sci China Phys Mech Astron* **2023**, *66* (4), 247211.
- (49) Peng, B. Monolayer Fullerene Networks as Photocatalysts for Overall Water Splitting. *J Am Chem Soc* **2022**, *144* (43), 19921–19931.
- (50) Tong, Y.; Liu, H.; Dai, S.; Jiang, D. Monolayer Fullerene Membranes for Hydrogen Separation. *Nano Lett* **2023**, *23* (16), 7470–7476.
- (51) Chang, X.; Liu, X.; Zheng, W.; Zhou, L.; Zhang, J. Monolayer Fullerene Network: A Promising Material for VOCs Sensor. *Appl Surf Sci* **2023**, *637*, 157909.
- (52) Kroto, H. W. The Stability of the Fullerenes C_n , with $n = 24, 28, 32, 36, 50, 60$ and 70 . *Nature* **1987**, *329* (6139), 529–531.
- (53) Khamatgalimov, A. R.; Kovalenko, V. I. Electronic Structure and Stability of C_{80} Fullerene IPR Isomers. *Fullerenes, Nanotubes and Carbon Nanostructures* **2011**, *19* (7), 599–604.
- (54) Zhao, Y.; Guo, Y.; Zhao, Y.; Yu, X.; Cherenda, N.; Su, Y.; Zhao, J. Two-Dimensional Fullerene-Based Monolayer Materials Assembled by C_{80} and $Sc_3N@C_{80}$. *Physical Chemistry Chemical Physics* **2024**, *26* (14), 10841–10849.
- (55) Khamatgalimov, A. R.; Luzhetskii, A. V.; Kovalenko, V. I. Unusual Pentagon and Hexagon Geometry of Three Isomers (No 1, 20, and 23) of Fullerene C_{84} . *Int J Quantum Chem* **2008**, *108* (8), 1334–1339.
- (56) Diener, M. D.; Alford, J. M. Isolation and Properties of Small-Bandgap Fullerenes. *Nature* **1998**, *393* (6686), 668–671.
- (57) Wang, T.; Wang, C. Endohedral Metallofullerenes Based on Spherical I_h-C_{80} Cage: Molecular Structures and Paramagnetic Properties. *Acc Chem Res* **2014**, *47* (2), 450–458.
- (58) Stevenson, S.; Rice, G.; Glass, T.; Harich, K.; Cromer, F.; Jordan, M. R.; Craft, J.; Hadju, E.; Bible, R.; Olmstead, M. M.; Maitra, K.; Fisher, A. J.; Balch, A. L.; Dorn, H. C. Small-Bandgap Endohedral Metallofullerenes in High Yield and Purity. *Nature* **1999**, *401* (6748), 55–57.
- (59) Wei, T.; Wang, S.; Lu, X.; Tan, Y.; Huang, J.; Liu, F.; Li, Q.; Xie, S.; Yang, S. Entrapping a Group-VB Transition Metal, Vanadium, within an Endohedral Metallofullerene: $V_xSc_{3-x}N@I_h-C_{80}$ ($x = 1, 2$). *J Am Chem Soc* **2016**, *138* (1), 207–214.
- (60) Li, M.; Zhao, Y.; Yuan, K.; Zhao, R.; Zhao, P.; Zhao, X. Insight into the Thermodynamically Preferred $V_3N@I(31924)-C_{80}$ and Acknowledged $V_xSc_{3-x}N@I(31924)-C_{80}$ ($X=0, 1$ and 2). *Carbon N Y* **2018**, *132*, 312–322.
- (61) Bhusal, S.; Baruah, T.; Yamamoto, Y.; Zope, R. R. Electronic Structure Calculation of Vanadium-and Scandium-based Endohedral Fullerenes $VSc_2N@C_{2n}$ ($2n = 70, 76, 78, 80$). *Int J Quantum Chem* **2018**, *118* (24).
- (62) Huang, B.; Clark, G.; Navarro-Moratalla, E.; Klein, D. R.; Cheng, R.; Seyler, K. L.; Zhong, D.; Schmidgall, E.; McGuire, M. A.; Cobden, D. H.; Yao, W.; Xiao, D.; Jarillo-Herrero, P.; Xu, X. Layer-Dependent Ferromagnetism in a van Der Waals Crystal down to the Monolayer Limit. *Nature* **2017**, *546* (7657), 270–273.
- (63) Kresse, G.; Furthmüller, J. Efficient Iterative Schemes for *Ab Initio* Total-Energy Calculations Using a Plane-Wave Basis Set. *Phys Rev B* **1996**, *54* (16), 11169–11186.
- (64) Kresse, G.; Joubert, D. From Ultrasoft Pseudopotentials to the Projector Augmented-Wave Method. *Phys Rev B* **1999**, *59* (3), 1758–1775.
- (65) Perdew, J. P.; Burke, K.; Ernzerhof, M. Generalized Gradient Approximation Made Simple. *Phys Rev Lett* **1996**, *77* (18), 3865–3868.

- (66) Grimme, S.; Antony, J.; Ehrlich, S.; Krieg, H. A Consistent and Accurate *Ab Initio* Parametrization of Density Functional Dispersion Correction (DFT-D) for the 94 Elements H-Pu. *J Chem Phys* **2010**, *132* (15), 154104.
- (67) Henkelman, G.; Arnaldsson, A.; Jónsson, H. A Fast and Robust Algorithm for Bader Decomposition of Charge Density. *Comput Mater Sci* **2006**, *36* (3), 354–360.
- (68) Soler, J. M.; Artacho, E.; Gale, J. D.; García, A.; Junquera, J.; Ordejón, P.; Sánchez-Portal, D. The SIESTA Method for *Ab Initio* Order- *N* Materials Simulation. *Journal of Physics: Condensed Matter* **2002**, *14* (11), 2745–2779.
- (69) García, A.; Papior, N.; Akhtar, A.; Artacho, E.; Blum, V.; Bosoni, E.; Brandimarte, P.; Brandbyge, M.; Cerdá, J. I.; Corsetti, F.; Cuadrado, R.; Dikan, V.; Ferrer, J.; Gale, J.; García-Fernández, P.; García-Suárez, V. M.; García, S.; Huhs, G.; Illera, S.; Korytár, R.; Koval, P.; Lebedeva, I.; Lin, L.; López-Tarifa, P.; Mayo, S. G.; Mohr, S.; Ordejón, P.; Postnikov, A.; Pouillon, Y.; Pruneda, M.; Robles, R.; Sánchez-Portal, D.; Soler, J. M.; Ullah, R.; Yu, V. W.; Junquera, J. Siesta : Recent Developments and Applications. *J Chem Phys* **2020**, *152* (20).
- (70) He, X.; Helbig, N.; Verstraete, M. J.; Bousquet, E. TB2J: A Python Package for Computing Magnetic Interaction Parameters. *Comput Phys Commun* **2021**, *264*, 107938.
- (71) Evans, R. F. L.; Fan, W. J.; Chureemart, P.; Ostler, T. A.; Ellis, M. O. A.; Chantrell, R. W. Atomistic Spin Model Simulations of Magnetic Nanomaterials. *Journal of Physics: Condensed Matter* **2014**, *26* (10), 103202.